Electron Spin Resonance Studies of One-electron Reduction Products of Nickel(II) and Palladium(II) Complexes containing Tetrathiomolybdate, Tetrathiotungstate, and Dialkyldithiocarbamate Ligands, $[M(M'S_4)_n(R_2NCS_2)_{2-n}]^{n-}$ (n = 0—2, M = Ni or Pd, M′ = Mo or W)†

Graham A. Bowmaker, Peter D. W. Boyd,* Graeme K. Campbell, and Maruta Zvagulis
Chemistry Department, University of Auckland, Auckland, New Zealand

The redox properties of nickel(II) and palladium(II) complexes of the type $[M(M'S_4)_n(R_2NCS_2)_{2-n}]^{n-}$ (n = 0—2, M = Ni or Pd, M′ = Mo or W) have been studied using d.c. and a.c. cyclic voltammetry at a platinum electrode in dichloromethane solution. The series of complexes show initial reversible or quasi-reversible one-electron reduction to give species containing a single unpaired electron. E.s.r. spectra have been used to identify the species produced after one-electron reduction. In the case of palladium, the reduction potential increases smoothly with increasing n whilst the unpaired electron is increasingly delocalised from the central metal ion with decreasing g anisotropy. In contrast, the reduction potential of the nickel complexes increases sharply from n = 0 to 1 with a corresponding increase in the g anisotropy. The reduction potential increases again for n = 2, however the e.s.r. spectrum shows an unusual 'reversal' of g anisotropy ($g_{\parallel} < g_{\perp}$) compared to that expected for a d^9 planar complex with the unpaired electron in a nickel d_{xy} orbital ($g_{\parallel} > g_{\perp}$). It is suggested that in the case of n = 1 or 2 the unpaired electron is now occupying a molecular orbital composed of the low-lying molybdenum (or tungsten) d orbitals. This is supported by scattered wave Xα calculations of the electronic structure of the model complexes $[Ni(H_2NCS_2)_2]$, $[Ni(MoS_4)(H_2NCS_2)]^-$ and $[Ni(MoS_4)_2]^{2-}$ and their one-electron reduction products.

Electrochemical and spectroscopic studies of transition-metal complexes of 1,1 dithio ligands such as dialkyldithiocarbamates (R_2NCS_2) and xanthates ($ROCS_2$) have shown that the metal d valence electrons are significantly delocalised onto the neighbouring sulphur-ligand atoms. In the well studied case of copper(II) bis(dialkyldithiocarbamates) $[Cu(R_2NCS_2)_2]$ the unpaired electron is about 53% delocalised from the metal d orbital,[1] whilst for the initial reduction product of nickel(II) bis(dialkyldithiocarbamates) $[Ni(R_2NCS_2)_2]^-$ this delocalisation is reduced to about 20%.[2] The unpaired electrons in both these molecules are considered to occupy 'metal-based' orbitals leading to their formulation as complexes of copper(II) and nickel(I) respectively.

The tetrathiometalate anions MS_4^{2-} (M = Mo or W), when complexed to nickel(II), palladium(II), and platinum(II), may also act as bidentate 1,1 dithio ligands.[3,4] The complexes which are formed are planar diamagnetic molecules of the form $[M(M'S_4)_2]^{2-}$ (M = Ni^{II}, Pd^{II}, or Pt^{II}; M′ = Mo or W). A feature of the tetrathiometalate ligand is the presence of unoccupied d orbitals on the metal of comparable energy to the valence orbitals of the central metal M. These orbitals may allow delocalisation of electron density from this central metal to M′.[5] The redox properties of these tetrathiometalate complexes have recently been reported by Callahan and Piliero.[4] The nickel(II) and palladium(II) complexes both undergo reversible one-electron reductions to give the trianionic $[M(M'S_4)_2]^{3-}$ at potentials of about −0.54 and −1.07 V respectively. These potentials are relatively insensitive to the tetrathiometalate ligand. The difference in reduction potential between the nickel and palladium complexes suggested that the initial reduction was based on the d^8 metal ion and that the unpaired electron occupied a b_{1g} (d_{xy}) molecular orbital (m.o.). These workers attempted to identify the one-electron reduction product of $[Ni(WS_4)_2]^{2-}$, generated chemically by $NaBH_4$ reduction, by e.s.r. spectroscopy. No signals were observed at room or liquid-nitrogen temperatures, but it is not clear whether this procedure produces the one- or two-electron reduction product.

An e.s.r. study of the one-electron reduction products of the nickel and palladium bis(tetrathiometalate) complexes generated by *in situ* controlled-potential electrolysis and a comparison with the analogous reduction products of the dialkyldithiocarbamate complexes, together with results on the mixed-ligand dithiocarbamate–tetrathiometalate complexes reported by Callahan and Cichon,[5] is presented in this work.

Experimental

The complexes $[NPr_4]_2[Ni(MoS_4)_2]$, $[NPr_4]_2[Ni(WS_4)_2]$, $[NPr_4]_2[Pd(MoS_4)_2]$, and $[NPr_4]_2[Pd(WS_4)_2]$ were prepared as described by Callahan and Piliero[4] by the reaction of $NiCl_2{\cdot}6H_2O$ or $K_2[PdCl_4]$ with the appropriate ammonium tetrathiometalate and tetrapropylammonium bromide. All complexes were recrystallised from acetonitrile:[4] $[NPr_4]_2[Ni(MoS_4)_2]$, m.p. >300 °C (Found: C, 32.15; H, 6.60; S, 27.0. Calc. for $C_{24}H_{56}Mo_2N_2NiS_8$: C, 32.75; H, 6.40; S, 29.15%); $[NPr_4]_2[Ni(WS_4)_2]$, m.p. >320 °C (Found: S, 22.35. Calc. for $C_{24}H_{56}N_2NiS_8W_2$: S, 24.3%); $[NPr_4]_2[Pd(MoS_4)_2]$, m.p. 210—220 °C (Found: S, 26.95. Calc. for $C_{24}H_{56}Mo_2N_2PdS_8$: S, 27.65%); and $[NPr_4]_2[Pd(WS_4)_2]$, m.p. 270—271 °C (Found: S, 22.15. Calc. for $C_{24}H_{56}N_2PdS_8W_2$: S, 23.25%).

The complexes $[Ni(Bu_2NCS_2)_2]$ and $[Pd(Bu_2NCS_2)_2]$ (m.p. 108 °C; lit.,[7] 108 °C) were prepared by literature methods[6,7] and recrystallised from chloroform–light petroleum (b.p. 40—60 °C); $[Pd(R_2NCS_2)_2]$ (R = Et or benzyl) were supplied by

---

† *Supplementary data available* (No. SUP 56476, 6 pp.): scattered wave Xα orbital energies and populations. See Instructions for Authors, *J. Chem. Soc., Dalton Trans.*, 1986, Issue 1, pp. xvii—xx.

Non-S.I. unit employed: G = 10^{-4} T.

Mrs. J. Hope, Research School of Chemistry, Australian National University.

The tetrapropylammonium salts of the mixed-ligand complexes $[M(M'S_4)(Bu_2NCS_2)]^-$ were prepared by the method of Callahan and Cichon[5] and recrystallised from acetonitrile or acetone: $[NPr_4][Pd(MoS_4)(Bu_2NCS_2)]$, m.p. 134—136 °C (Found: C, 34.75; H, 6.35; N, 3.85; S, 26.75. Calc. for $C_{21}H_{46}MoN_2PdS_6$: C, 34.95; H, 6.45; N, 3.90; S, 26.65%) and $[NPr_4][Pd(WS_4)(Bu_2NCS_2)]$, m.p. 143—144 °C (Found: C, 32.5; H, 6.10; N, 3.60; S, 23.85. Calc. for $C_{21}H_{46}PdS_6W$: C, 31.15; H, 5.75; N, 3.45; S, 23.75%).

Electron spin resonance spectra, electrochemical measurements, and irradiation experiments were performed as reported previously.[2] E.s.r. spectra were digitised through an interface from a Varian E4 spectrometer to a 10-bit analog-to-digital converter (ADC) to a CBM 3032 Pet microcomputer. The ADC monitored a filtered output voltage between the amplifier and pen recorder of the spectrometer. Digitised spectra so obtained could be corrected for sloping baselines. Integrated and second-derivative spectra could be calculated numerically on the microcomputer. These numerical spectra were used for comparison with simulated spectra.

Computational Methods.—All SCF-Xα-scattered wave calculations[8] were performed using the program XASW of Case and Cook[9–11] on the University of Auckland IBM 4341 computer. The structures for both nickel bis(dithiocarbamate) $[Ni(H_2NCS_2)_2]$[12] and nickel bis(tetrathiomolybdate) $[Ni(MoS_4)_2]^{2-}$[13] were idealised to D_{2h} symmetry from the reported crystal structures. The structure of the mixed-ligand complex $[Ni(MoS_4)(H_2NCS_2)]^-$ was taken as a composite of these two structures. The starting molecular potentials were constructed from a superposition of atomic charge densities using overlapping atomic spheres. The atomic radii were chosen using the method of Norman[14] as the atomic number radii reduced by a factor of 0.88. The co-ordinates, atomic radii, and values used in these calculations are given in Table 1. Partial wave expansions in each calculation were limited to $l = 4$ for the outer sphere, $l = 2$ for nickel and molybdenum, $l = 1$ for carbon, nitrogen, and sulphur, and $l = 1$ for hydrogen. In the case of the nickel bis(tetrathiomolybdate) dianion and nickel tetrathiomolybdate dithiocarbamate anion, Watson spheres of opposite charge with radius equal to the outer-sphere radius were used. The SCF-Xα-scattered wave calculation was continued until the relative change in potential at all points in the molecule was less than 10^{-4}. Charge distributions were calculated according to the method of Case, Cook, and Karplus.[10,11]

Table 1. Co-ordinates* and radii* used in calculations

Atom	*x*	*y*	*z*	Radius
$[Ni(H_2NCS_2)_2]$				
OUT	0	0	0	10.0377
Ni	0	0	0	2.3295
S	−2.6494	3.2409	0	2.3446
N	0	7.6327	0	1.6721
C	0	5.0343	0	1.6844
H	−1.6913	8.6721	0	1.2022
$[Ni(MoS_4)_2]^{2-}$				
OUT	0	0	0	10.8702
Ni	0	0	0	2.3178
Mo	0	5.3139	0	2.4472
S_B	−3.2666	2.6594	0	2.4635
S_T	0	7.6536	3.3229	2.5264
$[Ni(MoS_4)(H_2NCS_2)]^-$				
OUT	0	0	1.3907	10.3829
Ni	0	0	1.9257	2.3238
Mo	0	0	−3.3882	2.4474
S_D	0	−2.6494	5.1666	2.3421
N	0	0	9.5584	1.6721
C	0	0	6.9600	1.6844
H	0	−1.6913	10.5978	1.2022
S_B	0	3.2670	−0.7343	2.4746
S_T	3.3230	0	−5.7283	2.5266

* In atomic units, 1 Bohr = 52.918 pm; OUT = outer sphere.

Results and Discussion

Reduction of $[NPr_4]_2[Ni(MoS_4)_2]$ *and* $[NPr_4]_2[Ni(WS_4)_2]$.—The bis(tetrathiometalate) complexes of nickel(II) have been shown by Callahan and Piliero to undergo two reversible one-electron reductions at platinum electrodes in dimethylformamide solvent.

In studies performed here using platinum-disk electrodes and dichloromethane solvent, only the first reduction in the cyclic voltammogram, at −0.65 and −0.66 V for the molybdate and tungstate respectively, was readily observed. The second reduction merged with the solvent reduction wave. The relative redox potentials of the initial reduction agree well with those previously reported although their magnitudes differ due to different referencing, Table 2.

E.S.R. Spectra of Reduced $[Ni(MS_4)_2]^{2-}$ (M = Mo *or* W) *Complexes.*—E.s.r. spectra of frozen dichloromethane or dimethylformamide solutions formed after *in situ* controlled-potential electrolysis at the first reduction potential of the thiomolybdate and thiotungstate complexes consisted of strong broad signals in the $g \sim 2$ region. No room-temperature solution spectra for these species could be observed, Figure 1. The spectra varied only slightly for samples differing in concentration and method of preparation. Similar spectra at 77 K were observed on reduction of dimethylformamide solutions of $[Ni(WS_4)_2]^{2-}$ with $NaBH_4$.

All spectra showed an extended tail to low field which varied slightly with solvent. However, it appears to be part of the spectrum of the same species. Evidence for this was found from the spectra of frozen solutions of the nickel(II) complexes that had been γ-irradiated. Electrons ejected from the solvent matrix may be trapped by the solute complex leading to a reduced complex similar to the electrochemically produced initial

Table 2. Cyclic voltammetry parameters for the initial reduction of complexes $[NPr_4]_n[M(M'S_4)_n(Bu_2NCS_2)_{2-n}]$ (*n* = 0—2, M = Ni or Pd, M′ = Mo or W)[a]

Complex	$E_r^{0\,b}$/V	$\Delta E_{pp}{}^c$	$i_p{}^r/i_p{}^{f\,c}$
$[Ni(MoS_4)_2]^{2-}$	−0.65	0.150	0.96
$[Ni(WS_4)_2]^{2-}$	−0.66	0.100	0.91
$[Pd(MoS_4)_2]^{2-}$	−1.06	0.075	0.61
$[Pd(WS_4)_2]^{2-}$	−1.14	0.110	0.87
$[Ni(Bu_2NCS_2)_2]$	−1.61	0.140[d]	0.94[d]
$[Pd(Bu_2NCS_2)_2]$	−1.56	0.114[d]	0.77[d]
$[Pd(Et_2NCS_2)_2]$	−1.56	0.131	0.67
$[Pd\{(PhCH_2)_2NCS_2\}_2]$	−1.40	0.076	0.83
$[Ni(MoS_4)(Bu_2NCS_2)]^-$	−0.96	0.200	1.09
$[Ni(WS_4)(Bu_2NCS_2)]^-$	−0.96	0.150	0.90
$[Pd(MoS_4)(Bu_2NCS_2)]^-$	−1.25	0.075	0.58
$[Pd(WS_4)(Bu_2NCS_2)]^-$	−1.36	0.110	0.72

[a] In CH_2Cl_2 solvent. [b] Relative to ferrocene–ferrocenium oxidation at +0.46 V. Potential measured halfway between anodic and cathodic peaks. [c] Scan rate 20 mV s^{-1}. [d] Scan rate 200 mV s^{-1}, acetone solvent.

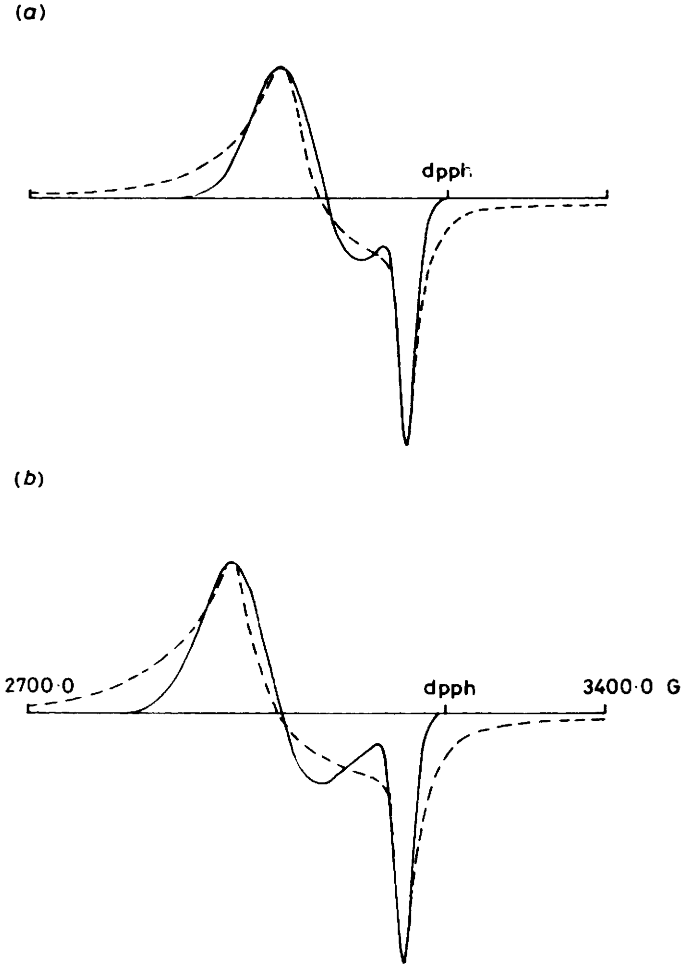

Figure 1. E.s.r. spectra of frozen dimethylformamide solutions of (*a*) reduced $[Ni(MoS_4)_2]^{2-}$ (– – –, observed; ——, calculated for $g_1 = 2.12$, $g_2 = 2.12$, $g_3 = 2.035$, $\sigma_1 = 41.0$, $\sigma_2 = 41.0$, and $\sigma_3 = 9.1$ G) and (*b*) reduced $[Ni(WS_4)_2]^{2-}$ at −160 K (– – –, observed; ——, calculated for $g_1 = 2.16$, $g_2 = 2.16$, $g_3 = 2.036$, $\sigma_1 = 46.0$, $\sigma_2 = 46.0$, and $\sigma_3 = 10.0$ G)

reduction product. The spectrum of this species in the low-field region still shows an extended tail very similar to that found for the electrochemically produced species in dimethylformamide.

The e.s.r. spectra of both the tetrathiomolybdate and tetrathiotungstate complexes may be interpreted as those of an axially symmetric $S = \frac{1}{2}$ species with $g_{\parallel} < g_{\perp}$. Simulations account for the principal features of the spectrum, but exact matching of the calculated and observed line slopes in the low-field region was not possible, Table 3(*a*). Alternative simulations with $g_{\parallel} > g_{\perp}$ were not able to account for the relative intensities of the peaks in the e.s.r. spectra in particular. The intensity of the lower-field peaks is too large for both complexes to be due to a '$g_{\parallel}$' feature of an $S = \frac{1}{2}$ spectrum. The tail to low field is most probably due to unresolved ^{95,97}Mo or ^{183}W hyperfine interaction.

The e.s.r. spectrum of the one-electron reduction product, $[^{61}Ni(WS_4)_2]^{3-}$, was identical in the high-field ($g_{\parallel}$) region with a slight broadening in the low-field ($g_{\perp}$) region which if due to ^{61}Ni hyperfine interactions would correspond to a coupling constant of less than 15×10^{-4} cm^{-1}. No evidence was found for spectra of the type observed for the reduced forms of $[^{61}Ni(Bu_2NCS_2)_2]$.[2]

E.S.R. Spectra of Reduced $[Pd(MS_4)_2]^{2-}$ (M = Mo *or* W) *Complexes*.—Controlled-potential electrolysis at the first reduction potential of the palladium tetrathiometalate complexes gave a species that was e.s.r. active in solution at room temperature and in frozen solution, unlike the analogous nickel species. The solution e.s.r. spectrum consisted of a strong central line at $g \sim 2$ together with satellite lines due to hyperfine interaction of the unpaired electron with ^{105}Pd (22.23%, $I = \frac{5}{2}$), Table 3(*a*). The isotropic *g* value for the thiomolybdate complex (2.004) was very close to that of diphenylpicrylhydrazyl (dpph) and that for the thiotungstate complex was 2.022. Frozen-solution spectra were anisotropic, Figure 2, with *g* values of near axial symmetry. These spectra also showed lines due to electron hyperfine interaction with the ^{105}Pd nucleus. Simulation of the spectra was attempted using a model including the 22.23% of the palladium isotope. The features due to the $I = 0$ isotope could be well reproduced in the simulation with near axial symmetry ($g_{\parallel} > g_x \approx g_y$). However it was more difficult to obtain values of the anisotropic hyperfine interaction due in part to the overlap of hyperfine lines and the incomplete resolution of the spectrum. Thus the simulations shown in Figure 2 are only for the $I = 0$ isotope of Pd.

Reduction of $[Pd(R_2NCS_2)_2]$ *Complexes*.—Several bis(dithiocarbamato) complexes of palladium have been shown by van der Linden and Dix[15] to undergo a quasi-reversible one-electron reduction at a platinum electrode in acetone solvent to give unstable $[Pd(R_2NCS_2)_2]^-$ complexes. The reduction of the same complexes was observed in the present work using a platinum-disk electrode and dichloromethane or acetone solvent, and the cyclic voltammetry parameters are given in Table 2. These reductions occur at more negative potentials and have larger cathodic-to-anodic peak separations than those of the corresponding nickel(II) complexes. This suggests that the palladium dithiocarbamates have slower electron-transfer rates than the corresponding nickel complexes. A.c. voltammetric experiments show that the electron transfer is completely reversible, however, Figure 3.

E.S.R. Spectra of Reduced $[Pd(R_2NCS_2)_2]$ *Complexes*.—The *in situ* reduction of the palladium dithiocarbamate complexes $[Pd(R_2NCS_2)_2]$ (R = Bu, CH_2Ph, C_6H_{11}, or Et) at −40 °C in dichloromethane resulted in strong e.s.r. signals. Due to the broadness of the lines ($\sigma = 46$ G) no ^{105}Pd satellite lines were evident in the solution spectra. The e.s.r. spectra of the frozen solutions at 77 K are typical of axially symmetric $S = \frac{1}{2}$ systems, although a slight rhombic distortion was generally observed. A decrease in linewidth in these spectra led to a resolution of ^{105}Pd satellite lines in both the parallel and perpendicular regions. The frozen-solution spectrum of $[Pd(Bu_2NCS_2)_2]^-$ is shown in Figure 4, and the e.s.r. spin-Hamiltonian parameters for all $[Pd(R_2NCS_2)_2]^-$ species studied in this work are given in Table 3(*b*).

E.s.r. spectra have been reported for a variety of palladium complexes produced by γ-irradiation at 77 K of powders or glassy solutions of palladium complexes. In order to see whether bis(dithiocarbamato)palladium(I) complexes could be generated in this manner, a frozen solution of $[Pd(Bu_2NCS_2)_2]$ in xylene was γ-irradiated at 77 K using the experimental conditions previously described in a similar study of some nickel(II) dithiocarbamates.[2] A weak signal was observed which was identical to the one obtained in the electrochemical reduction, Table 3(*b*).

The species generated in the γ-irradiation experiments is expected to have the same geometrical structure as that of the palladium(II) complex. The above result suggests that the quasi-reversible electrochemical reduction simply involves electron transfer without any change in structure relative to the four-co-

Table 3. E.s.r. parameters

(*a*) For reduction products[a]

Parent complex	g_{iso}	g_1	g_2	g_3	a[b]	A_1[b]	A_2[b]	A_3[b]
$[Ni(MoS_4)_2]^{2-}$[c]	—	2.121	2.121	2.035	—	—	—	—
$[Ni(WS_4)_2]^{2-}$[c]	—	2.159	2.159	2.036		—	—	—
$[Pd(MoS_4)_2]^{2-}$	2.004	2.033	2.004	2.002	21.5			
$[Pd(WS_4)_2]^{2-}$	2.022	2.052	2.013	2.007	20.8			
$[Ni(Bu_2NCS_2)_2]$[d]	—	2.272	2.062	2.062	—	53	8	8
$[Pd(Bu_2NCS_2)_2]$	2.076[e]	2.202	2.044	2.037	[f]	43.7	24.7	25.2
$[Ni(MoS_4)(Bu_2NCS_2)]^-$	2.180	2.357	2.116	2.064				
$[Ni(WS_4)(Bu_2NCS_2)]^-$	—	2.386	2.131	2.055				
$[Pd(MoS_4)(Bu_2NCS_2)]^-$	2.031	2.037	2.025	2.018	26.0			
$[Pd(WS_4)(Bu_2NCS_2)]^-$	2.040	2.064	2.046	2.028	24.4			

(*b*) For $[Pd^I(R_2NCS_2)_2]^-$ and related complexes

Complex	g[g]	g_1	g_2	g_3	A_1[b]	A_2[b]	A_3[b]
$[Pd(Bu_2NCS_2)_2]^-$[h]	2.076	2.202	2.044	2.037	43.7	24.7	25.2
$[Pd(Bu_2NCS_2)_2]^-$[i]		2.209	2.046	2.040	—	—	—
$[Pd\{(PhCH_2)_2NCS_2\}_2]^-$[h]	2.080	2.194	2.045	2.037	44.0	24.6	25.0
$[Pd\{(C_6H_{11})_2NCS_2\}_2]^-$[h]	2.075	2.192	2.043	2.036	43.5	24.7	24.9
$[Pd(Et_2NCS_2)_2]^-$[h]	2.084	2.203	2.044	2.036	44.3	24.7	25.2
$[Pd(mnt)_2]^{3-}$[j]		2.116	2.042	2.034	44	29	26
$[PdCl_4]^{3-}$[k]		2.515	2.084	2.084	35.7	24.7	24.7
$[Ag^{II}(Pr^i_2NCS_2)_2]$[l]		2.035	2.011	2.011	−37	−24	−24

[a] In CH_2Cl_2 solution. [b] $\times 10^4$, cm^{-1}. [c] In dimethylformamide solution. [d] Ref. 2, species I. [e] Solution spectrum at −40 °C. [f] Not resolved. [g] Solution spectrum value, at −40 °C. [h] Hyperfine coupling constants A_2 and A_3 were estimated by measuring the positions of lines 1 and 6 for each sextet, and dividing the spacing by five. [i] Generated by γ-irradiation in *o*-, *m*-, and *p*-xylene. Hyperfine structure not observed. [j] Ref. 16. [k] T. Krigas and M. T. Rogers, *J. Chem. Phys.*, 1971, **54**, 4769. [l] R. Aasa, R. Petterson, and T. Vänngard, *Nature (London)*, 1961, **110**, 258.

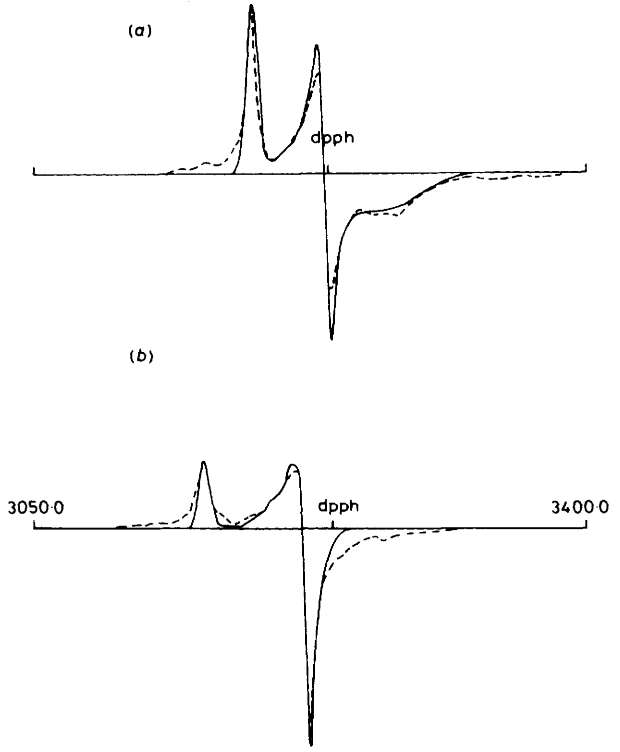

Figure 2. E.s.r. spectra of frozen dichloromethane solutions of (*a*) reduced $[Pd(MoS_4)_2]^{2-}$ (– – –, observed; ——, calculated for g_1 = 2.033, g_2 = 2.004, g_3 = 2.002, σ_1 = 2.0, σ_2 = 6.5, and σ_3 = 5.4 G) and (*b*) reduced $[Pd(WS_4)_2]^{2-}$ at −160 K (– – –, observed; ——, calculated for g_1 = 2.052, g_2 = 2.013, g_3 = 2.007, σ_1 = 3.3, σ_2 = 1.5, and σ_3 = 9.0 G)

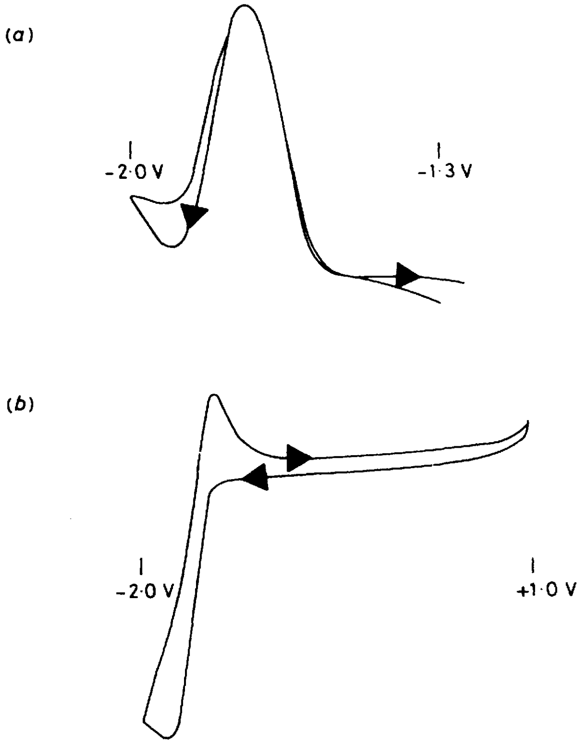

Figure 3. (*a*) A.c. cyclic voltammogram of the reduction of $[Pd(Bu_2NCS_2)_2]$ in dichloromethane, 0.1 mol dm^{-3} NBu_4ClO_4. Modulation: 400 Hz, 5 mV. Scan rate 10 mV s^{-1}. (*b*) D.c. cyclic voltammogram of the reduction of $[Pd(Bu_2NCS_2)_2]$ in the same solvent. Scan rate 100 mV s^{-1}

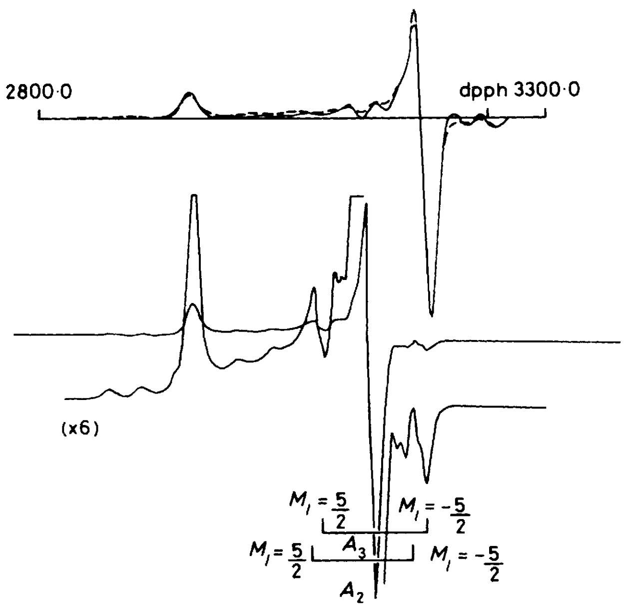

Figure 4. E.s.r. spectrum of a frozen dichloromethane solution of reduced $[Pd(Bu_2NCS_2)_2]$ (– – –, observed; ——, calculated for g_1 = 2.202, g_2 = 2.044, g_3 = 2.037, $A_1 = 43.7 \times 10^{-4}$, $A_2 = 24.7 \times 10^{-4}$, $A_3 = 25.2 \times 10^{-4}$ cm^{-1}, $\sigma_1 = 8.0$, $\sigma_2 = 5.0$, and $\sigma_3 = 5.0$ G). Lower part of figure shows the expanded experimental spectrum with resolved perpendicular hyperfine features

ordinate planar complex $[Pd(Bu_2NCS_2)_2]$. This species is thus analogous to the first species formed in the one-electron reduction of the nickel dithiocarbamates $[Ni(R_2NCS_2)_2]^-$. In the case of the nickel compounds it was found that the first formed species undergoes a transformation to a second paramagnetic species which was detected by the growth of a second e.s.r. signal with 'reversed' g values ($g_{\parallel} < g_{\perp}$). No such species were detected in the case of the reduced palladium compounds, which appear to decompose or react to give e.s.r.-inactive products exclusively.

Four of the six expected ^{105}Pd hyperfine lines were seen in the parallel and perpendicular regions, the centre two lines being obscured by the strong signals due to complexes containing the non-magnetic palladium isotopes. The palladium satellite lines in the perpendicular region showed slight irregularities in position and intensity which could not be accounted for in the spectral simulation using any combination of g values and hyperfine coupling constants, with either coincident or non-coincident principal axes for the g and hyperfine tensors. Geiger and co-workers[16] have observed a similar effect in the ^{105}Pd satellites in the perpendicular region in the frozen-solution spectrum of $[Pd(mnt)_2]^{3-}$ (mnt = maleonitriledithiolate), and have suggested that it may be due to a small quadrupole interaction involving the ^{105}Pd nucleus.

An estimate of the covalency parameter α^2 for the metal–ligand bonding in the $[Pd(R_2NCS_2)_2]^-$ species can be obtained from the hyperfine coupling constants and g values by the method described previously for the corresponding nickel complexes.[2] For $[Pd(Bu_2NCS_2)_2]^-$ with $A_{\parallel}$ ($= A_1$) and $A_{\perp}$ [$= (A_2 + A_3)/2$] both positive and the dipolar electron nuclear coupling constant $P_0(^{105}Pd) = -58 \times 10^{-4}$ cm^{-1},[17] $\alpha^2 = 0.60$. All other possibilities for the signs of the hyperfine coupling constants give unreasonable results. The values obtained indicate that the unpaired electron is about 60% located in the 4*d* orbital of the Pd atom, and that the complex is thus properly regarded as one of Pd^I. A comparison can be made between this α^2 value and those for the related complexes listed in Table 4. It is close to those found for several other palladium complexes, but larger than that for the isoelectronic $[Ag^{II}(Pr^i{}_2NCS_2)_2]$. This indicates a greater degree of metal–ligand covalency in the silver complex and is similar to the situation previously found in a comparison of related dithiocarbamates of Ni and Cu.[2] The degree of covalency in $[Pd(Bu_2NCS_2)_2]^-$ is significantly larger than that in the corresponding nickel complex. This indicates a greater degree of delocalisation of the unpaired electron onto the ligands in the case of the palladium complex and is consistent with the observation that the g values for the palladium complexes are closer to the free-electron value than those of the nickel complexes. It also suggests a possible explanation for the lack of observation of a second paramagnetic species in the electrochemical generation of the $[Pd(R_2NCS_2)_2]^-$ species. In the case of the corresponding nickel(I) complex where this was observed, it was attributed to a one-ended dissociation of the dithiocarbamate ligand to produce a nickel(I) complex with a co-ordination number less than four.[2] It is possible that the greater metal–ligand covalency observed in the case of the palladium(I) complexes is sufficient to prevent this from occurring in these compounds.

Table 4. Calculated covalency parameters α^2

Complex	Method of generation	α^2
$[Ni(Bu_2NCS_2)_2]^-$	Electrolysis, irradiation[2]	0.80
$[Ni(mnt)_2]^{3-}$	Electrolysis[16]	0.75
$[Pd(Bu_2NCS_2)_2]^-$	Electrolysis, irradiation[a]	0.60
$[Pd(SCN)_4]^{3-}$	Irradiation[b]	0.55
$[Pd(tu)_4]^{+}$[c]	Irradiation[b]	0.62
$[Cu(Et_2NCS_2)_2]$	Stable[1]	0.45
$[Ag(Pr^i{}_2NCS_2)_2]$	Stable[d]	0.45

[a] This work. [b] S. Funiwara and M. Nakamura, *J. Phys. Chem.*, 1974, **78**, 2136. [c] tu = Thiourea. [d] R. Petterson and T. Vanngard, *Ark. Kemi*, 1961, **17**, 249.

Reduction Electrochemistry of the Mixed-ligand Complexes $[M(M'S_4)(R_2NCS_2)]^-$ (M' = Mo *or* W, M = Ni *or* Pd).—Mixed-ligand complexes of the type $[M(M'S_4)(R_2NCS_2)]^-$ (M = Ni or Pd, M' = Mo or W) have been reported by Callahan and Cichon[5] and are planar diamagnetic four-co-ordinate complexes of the appropriate Group 8 metal. Cyclic voltammetry at platinum-disk electrodes in dichloromethane solvent, scanning initially to cathodic potentials, showed a reduction process and an associated anodic peak on return. The peak-to-peak separation in each case was greater than for an electrochemically reversible process and decreased with decreasing scan rate, Table 2, as might be expected for a quasi-reversible electrochemical process. Similar effects have been noted in other sulphur chelate systems that are reversibly oxidised or reduced chemically. The estimated formal potentials were as expected intermediate between those of the appropriate bis(tetrathiometalate) and bis(dialkyldithiocarbamate) complex.

E.S.R. Spectra of Reduced $[M(M'S_4)(R_2NCS_2)]^-$ (M = Ni *or* Pd, M' = Mo *or* W) *Complexes*.—E.s.r. spectra of dichloromethane solutions of $[Ni(M'S_4)(R_2NCS_2)]^-$ (M' = Mo or W) reduced by controlled-potential electrolysis gave a single line that decayed with time. Spectra of frozen solutions sampled at differing times during electrolysis indicated the presence of several e.s.r.-active species. However the dominant feature of the frozen-solution spectra of both compounds obtained as soon as possible after commencement of electrolysis was a strongly anisotropic rhombic spectrum, Table 2 and Figure 5. The averages of the g values for these species are greater

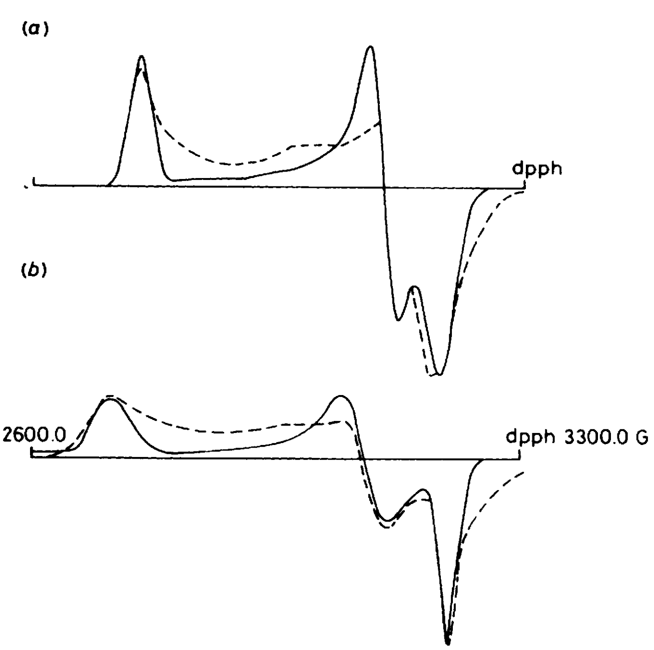

Figure 5. E.s.r. spectra of a frozen dichloromethane solution at −160 K of (*a*) reduced $[Ni(MoS_4)(Bu_2NCS_2)]^-$ (– – –, observed; ——, calculated for $g_1 = 2.357$, $g_2 = 2.116$, $g_3 = 2.064$, $\sigma_1 = 14.0$, $\sigma_2 = 14.0$, and $\sigma_3 = 18.0$ G) and (*b*) reduced $[Ni(WS_4)(Bu_2NCS_2)]^-$ (– – –, observed; ——, calculated for $g_1 = 2.386$, $g_2 = 2.131$, $g_3 = 2.055$, $\sigma_1 = 27.0$, $\sigma_2 = 23.0$, and $\sigma_3 = 12.0$ G)

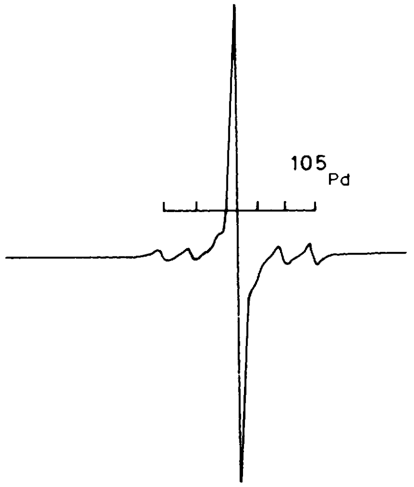

Figure 6. E.s.r. spectrum of a dichloromethane solution of reduced $[Pd(Bu_2NCS_2)_2]$ at room temperature

than those for the corresponding $[Ni(M'S_4)_2]^{3-}$ and $[Ni(Bu_2NCS_2)_2]^-$ species. In contrast the palladium complexes gave stable species in solution that were e.s.r. active. The spectra consisted of a central single line with six satellite lines due to the ^{105}Pd hyperfine interaction, Figure 6. Frozen-solution spectra, Figure 7, were anisotropic (rhombic) with g values intermediate between those for the corresponding $[Pd(M'S_4)_2]^{3-}$ and $[Pd(R_2NCS_2)_2]^-$ species. Simulations are given only for the $I = 0$ isotope.

The Nature of the Singly Occupied Molecular Orbital (s.o.m.o.) in Reduced Nickel and Palladium Thiomolybdates.— The variation of the first reduction potential E_0' with the number of MoS_4^{2-} groups in $[M(M'S_4)_n(Bu_2NCS_2)_{2-n}]^{n-}$ (M = Ni or Pd, M′ = Mo or W) is shown in Figure 8. From this it can be seen that the behaviour of the nickel and palladium complexes is fundamentally different. The palladium complexes show a regular increase in E_0' with n whilst the nickel complexes show a large increase between $n = 0$ and 1.

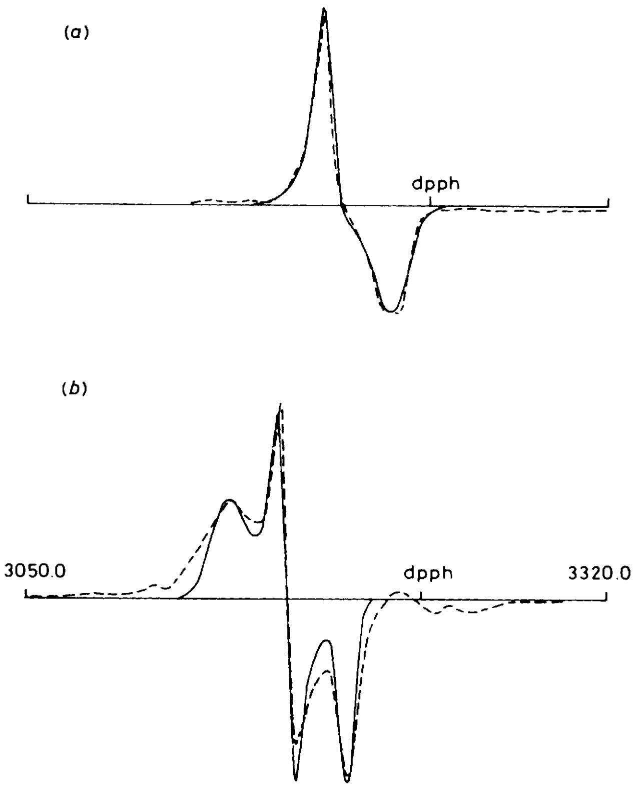

Figure 7. E.s.r. spectra of frozen dichloromethane solutions at −160 K of (*a*) reduced $[Pd(MoS_4)(Bu_2NCS_2)]^-$ (– – –, observed; ——, calculated for $g_1 = 2.037, g_2 = 2.025, g_3 = 2.018, \sigma_1 = 3.0, \sigma_2 = 6.5$, and $\sigma_3 = 5.3$ G) and (*b*) reduced $[Pd(WS_4)(Bu_2NCS_2)]^-$ (– – –, observed; calculated for $g_1 = 2.064$, $g_2 = 2.046$, $g_3 = 2.028$, $\sigma_1 = 20.2$, $\sigma_2 = 21.3$, and $\sigma_3 = 6.1$ G)

Consideration of the electrochemical and e.s.r. data shows that the behaviour of the palladium complexes can be understood in terms of an essentially palladium-based reduction, but with increasing delocalisation of the single electron onto the ligands with increasing n. This is qualitatively similar to our previous observations on the series of complexes $[Ni(dppe)_n(R_2NCS_2)_{2-n}]^{n+}$ (dppe = $Ph_2PCH_2CH_2PPh_2$), where increasing delocalisation from the nickel atom of the unpaired electron in the reduced species was associated with an increase in the reduction potential of the complex.[2]

The behaviour of the nickel complexes differs from this, however. The much greater ease of reduction of the mixed-ligand complex ($n = 1$ compared to $n = 0$) suggests that the added electron should be more strongly delocalised from the nickel in the $n = 1$ case. However, the average of the g values for the mixed-ligand complex is greater than that of $[Ni(Bu_2NCS_2)_2]^-$, implying either a greater localisation of the unpaired electron on the nickel atom or a change in the composition of the s.o.m.o. This is supported by the observation that the reduced nickel mixed-ligand complexes are so unstable that it is difficult to obtain a clean e.s.r. spectrum of them whilst the corresponding palladium complexes, which are much more stable, allow the recording of spectra free from decomposition products.

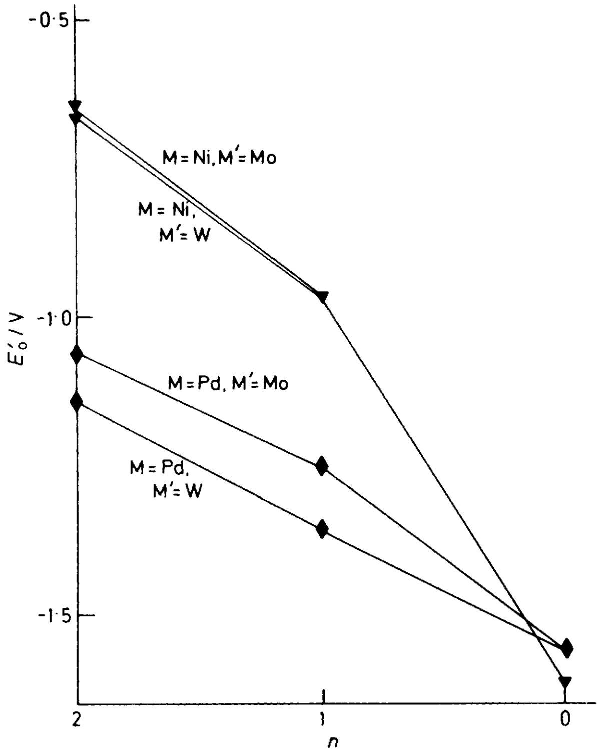

Figure 8. Variation of the first reduction potential as a function of *n* for complexes $[M(M'S_4)_n(Bu_2NCS_2)_{2-n}]^{n-}$ (M = Ni or Pd, M′ = Mo or W)

The *n* = 2 nickel complexes, $[Ni(MS_4)_2]^{2-}$, show particularly anomalous behaviour. They have the highest reduction potential of all the compounds studied in the present work. Despite this their reduction products are only moderately stable and their frozen-solution spectra show reversed *g* values ($g_{\parallel} < g_{\perp}$). These data then suggest that the site of reduction in the nickel *n* = 1 and 2 complexes containing the tetrathiomolybdate or tetrathiotungstate ligands is not at the nickel atom but rather at the Group 6 metal. A comparison of $[Ni(WS_4)_2]^{3}$ with $[Ni(MoS_4)_2]^{3-}$ shows an increasing anisotropy in keeping with the increased spin–orbit coupling of tungsten compared to molybdenum. In neither case, however, could $^{95,97}Mo$ or ^{183}W hyperfine be resolved due to the large linewidths in these spectra.

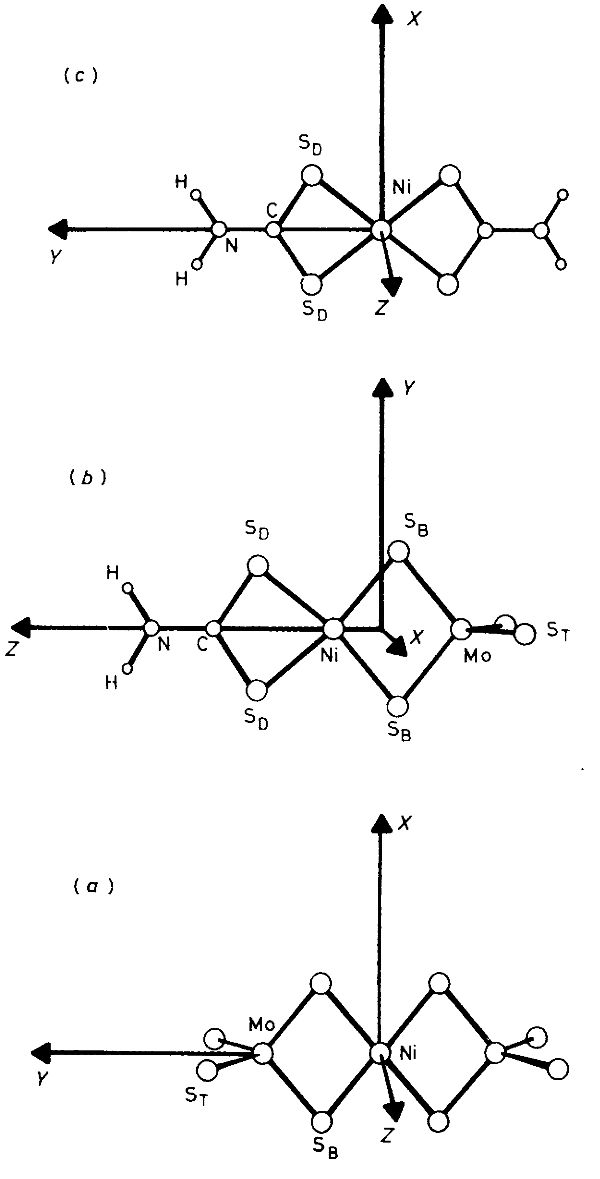

Figure 9. Co-ordinate schemes used in scattered wave Xα calculations of (*a*) $[Ni(MoS_4)_2]^{2-}$, (*b*) $[Ni(MoS_4)(H_2NCS_2)]^-$, and (*c*) $[Ni(H_2NCS_2)_2]$

Table 5. Gross orbital populations and atomic charges

	Ni			Mo			S_B		S_T		S_D		C		N		H
Molecule	*s*	*p*	*d*	*s*	*p*	*d*	*s*	*p*	*s*	*p*	*s*	*p*	*s*	*p*	*s*	*p*	*s*
$[Ni(H_2NCS_2)_2]$	0.625	0.666	9.124								1.708	4.489	1.128	2.543	1.372	3.764	0.796
(Charge)	(−0.415)										(−0.197)		(+0.329)		(−0.136)		(+0.204)
$[Ni(MoS_4)(H_2NCS_2)]^-$	0.609	0.682	9.058	0.477	0.538	4.343	1.818	4.486	1.834	4.637	1.713	4.441	1.131	2.549	1.372	3.773	0.805
(Charge)	(−0.349)			(+0.642)			(−0.304)		(−0.471)		(−0.154)		(+0.320)		(−0.145)		(+0.195)
$[Ni(MoS_4)_2]^{2-}$	0.581	0.676	9.057	0.483	0.538	4.348	1.839	4.445									
(Charge)	(−0.314)			(+0.631)			(−0.284)		(−0.453)								
$[MoS_4]^{2-}$				0.493	0.610	4.146	1.861	4.826									
(Charge)				(+0.751)			(−0.687)										

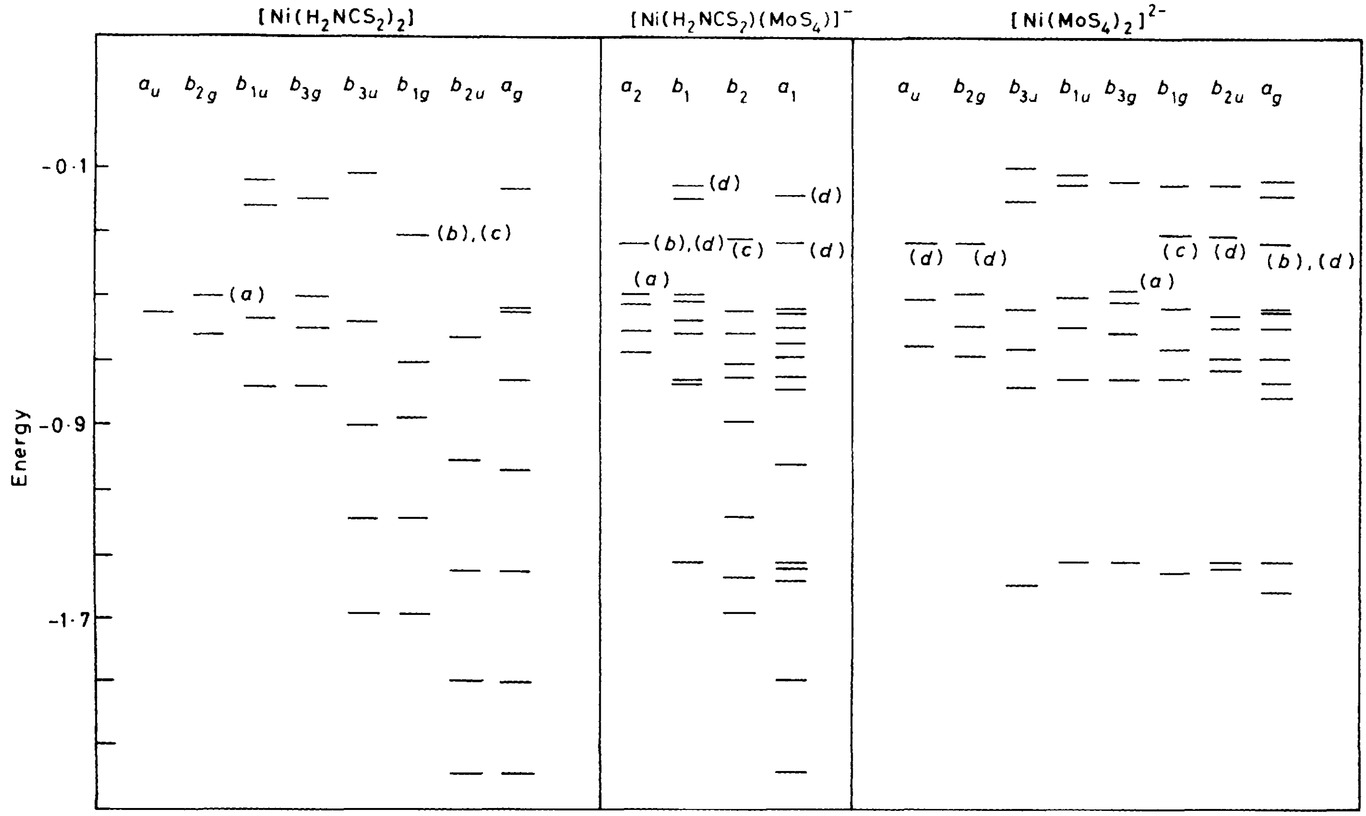

Figure 10. Scattered wave Xα orbital energies (atomic units): (*a*) highest occupied molecular orbital (h.o.m.o.); (*b*) l.u.m.o; (*c*) empty Ni $d_{xy(xz)}$ orbital; and (*d*) Mo *d* orbitals

Electronic Structures of $[Ni(H_2NCS_2)_2]$, $[Ni(MoS_4)_2]^{2-}$, *and* $[Ni(MoS_4)(H_2NCS_2)]^-$ *and their One-electron Reduction Products*.—Scattered wave Xα calculations of the electronic structures of $[Ni(H_2NCS_2)_2]$, Figure 9(*c*), $[Ni(MoS_4)_2]^{2-}$, Figure 9(*a*), and $[Ni(MoS_4)(H_2NCS_2)]^-$, Figure 9(*b*), were performed to obtain further information on the nature of the low-lying unoccupied orbitals of these complexes. Figure 10 shows the calculated energy-level schemes for each complex and Table 5 gives the populations of the higher-lying levels. An immediate feature of interest from these calculations is the position of low-lying unoccupied Mo *d* orbitals in both $[Ni(MoS_4)_2]^{2-}$ and $[Ni(MoS_4)(H_2NCS_2)]^-$. The 'normal' lowest unoccupied molecular orbital (l.u.m.o.) expected in planar nickel(II) complexes, the d_{xy} orbital,* is found to be at higher energies whilst for $[Ni(H_2NCS_2)_2]$ it is the l.u.m.o. This supports the suggestion in the previous section that the s.o.m.o. of the reduction products for $n = 1$ or 2 is predominantly based on the molybdenum atom. To investigate this calculations were performed on the complexes $[Ni(H_2NCS_2)_2]^-$, $[Ni(MoS_4)(H_2NCS_2)]^{2-}$, and $[Ni(MoS_4)_2]^{3-}$ with a single unpaired electron occupying the l.u.m.o. of the corresponding nickel(II) complex. The unoccupied orbitals are quite close together in energy for the thiomolybdate-containing molecules. Transition-state calculations [18] were performed to ensure that these configurations correspond to the ground state. In the case of the mixed-ligand complex the s.o.m.o. is principally composed of the molybdenum d_{xy} orbital (population 0.622) followed closely by the $14a_1$ orbital made up of molybdenum d_{z^2} and $d_{x^2-y^2}$ orbitals. Transition-state calculations on the complex $[Ni(MoS_4)(H_2NCS_2)]^{2-}$ indicate that the lowest s.o.m.o. corresponds to the $5a_2$ orbital of the oxidised complex. The l.u.m.o. of the complex $[Ni(MoS_4)_2]^{2-}$ is the $9a_g$ molecular orbital principally composed of the two molybdenum $d_{x^2-y^2}$ and d_{z^2} orbitals with the next highest empty orbital $4b_{2g}$ being composed of the two molybdenum d_{xy} orbitals. Again transition-state calculations show for the reduced complex that the $9a_g$ is the s.o.m.o. In both the bis- and mono-thiomolybdate complexes the nickel orbitals $5b_{1g}$ and $9b_2$ are at higher energies in both the oxidised and reduced species. These calculations then support the previous suggestion that the site of reduction for $[Ni(MoS_4)_2]^{2-}$ and $[Ni(MoS_4)(Bu_2NCS_2)]^-$ is at the molybdenum atom.

Conclusions

A combination of electrochemical, e.s.r. spectroscopic, and theoretical studies leads to the proposal that the initial one-electron reduction of nickel(II) tetrathiomolybdate (and tungstate) complexes occurs at the Group 6 metal atom unlike the previously well known reduction of nickel(II) to nickel(I) in a large variety of planar chelates of nickel with 1,1 and 1,2 dithio ligands.[2,16,19] This reduction of the 'ligand' rather than the central Group 8 metal has been observed recently in the case of nickel 1,3-dithio-β-diketonates.[20] In contrast the analogous palladium(II) complexes appear to undergo reduction principally at the palladium centre even in the case of the tetrathiometalate ligands, but with increasing delocalisation of the unpaired electron from the s.o.m.o. with increasing numbers of thiometalate ligands.

The large anisotropy in the *g* values for the reduced complexes of $[Ni(MoS_4)_2]^{3-}$ and $[Ni(MoS_4)(Bu_2NCS_2)]^{2-}$

---

* For the mixed-ligand complex (C_{2v} symmetry) the nickel l.u.m.o. is d_{xz}.

appears unusual at first sight for a molybdenum-based s.o.m.o. in comparison with corresponding molybdenum(V) complexes. However, the composition of this orbital as predicted from theoretical calculations does not correspond to the usual ground states found in such complexes.

Acknowledgements

We thank the Auckland University Grants Committee and New Zealand University Grants Committee for financial assistance. M. Z. acknowledges the receipt of an Auckland University Postdoctoral Fellowship.

References

1 T. R. Reddy and R. Srinivasan, *J. Chem. Phys.*, 1965, **43**, 1404.
2 G. A. Bowmaker, P. D. W. Boyd, G. K. Campbell, J. M. Hope, and R. L. Martin, *Inorg. Chem.*, 1982, **21**, 1152.
3 A. Muller, E. Diemann, R. Jostes, and H. Bogge, *Angew. Chem., Int. Ed. Engl.*, 1981, **20**, 934.
4 K. P. Callahan and P. A. Piliero, *Inorg. Chem.*, 1980, **19**, 2619.
5 K. P. Callahan and E. J. Cichon, *Inorg. Chem.*, 1981, **20**, 1941.
6 A. R. Hendrickson, R. L. Martin, and N. M. Rohde, *Inorg. Chem.*, 1975, **14**, 2980.
7 R. J. Magee and C. G. Sceney, *Inorg. Nucl. Chem. Lett.*, 1974, **10**, 323.
8 K. H. Johnson, *Adv. Quantum Chem.*, 1973, **7**, 143; J. C. Slater and K. H. Johnson, *Phys. Rev.*, 1972, **B5**, 844.
9 Program XASW, General Release VAX-IBM version no. 2, D. A. Case and M. Cook.
10 D. A. Case and M. Karplus, *Chem. Phys. Lett.*, 1976, **39**, 33.
11 D. A. Case, M. Cook, and M. Karplus, *J. Chem. Phys.*, 1980, **73**, 3294.
12 M. Bonamico, G. Dessy, C. Mariani, A. Vaciago, and L. Zambonelli, *Acta Crystallogr.*, 1965, **19**, 619.
13 I. Sotofte, *Acta Chem. Scand., Ser. A*, 1976, **30**, 157.
14 J. G. Norman, jun., *Mol. Phys.*, 1976, **31**, 1191.
15 J. G. M. van der Linden and A. H. Dix, *Inorg. Chim. Acta*, 1979, **35**, 65.
16 W. E. Geiger, C. S. Allen, T. E. Mines, and F. C. Senftlber, *Inorg. Chem.*, 1977, **16**, 2003.
17 B. A. Goodman and J. B. Raynor, *Adv. Inorg. Nucl. Chem.*, 1970, **13**, 135.
18 J. C. Slater, *Adv. Quantum Chem.*, 1972, **6**, 1.
19 G. A. Bowmaker, P. D. W. Boyd, and G. K. Campbell, *Inorg. Chem.*, 1982, **21**, 2403.
20 G. A. Bowmaker, P. D. W. Boyd, K. J. Cavell, A. F. Masters, and M. Zvagulis, *Inorg. Chem.*, 1985, **24**, 401.

Received 12*th February* 1985; *Paper* 5/249